Appl. Phys. A 81, 1619–1625 (2005)
DOI: 10.1007/s00339-005-3371-5

Applied Physics A
Materials Science & Processing

D. MACDONALD

Impact of nickel contamination on carrier recombination in *n*- and *p*-type crystalline silicon wafers

Department of Engineering, Faculty of Engineering and Information Technology,
The Australian National University, Canberra, ACT 0200, Australia

Received: 30 March 2005 / Accepted: 20 July 2005
Published online: 14 September 2005 • **© Springer-Verlag 2005**

ABSTRACT The effect of Ni surface contamination on carrier recombination after high temperature processing of crystalline silicon wafers has been studied for a range of *n*- and *p*-type resistivities. The results suggest that the presence of Ni precipitates at the wafer surfaces, formed during cooling, dominate the measured lifetimes. These precipitates exhibit a greater impact on the low-injection lifetime in *p*-type samples than in *n*-type. In addition, the injection-dependent lifetime curves for the *n*-type samples changed from increasing to decreasing with injection-level as the resistivity increased above approximately 10 Ω cm. In most cases, the surface recombination velocity attributable to the presence of these Ni precipitates at the oxidized surfaces increased linearly with the Ni dose.

PACS 72.20.Jv; 73.20.Hb; 71.55.Cn

1 Introduction

Nickel is a highly soluble and fast-diffusing metal impurity in crystalline silicon. It can arise as a surface contaminant during wafer processing [1, 2], and sometimes in significant concentrations during crystal growth of certain photovoltaic-grade materials [3–5]. As a surface impurity, it has the potential to penetrate deeply during device processing, and can quickly reach relatively high concentrations. Device performance may then be degraded through increased leakage currents and recombination.

Previous work on the electrical activity of Ni-related defects in silicon has predominantly been based on Deep-Level Transient Spectroscopy (DLTS) and its numerous variants [1, 6–9]. These studies have revealed a number of deep and shallow bands associated with precipitates, and other discrete levels attributed largely to substitutional Ni. For devices such as solar cells, however, it is important to know which of these levels are most active in terms of recombination. The most directly relevant parameter for assessing this is the carrier lifetime. Such lifetime studies in relation to Ni contamination are scarce, the most comprehensive apparently being those of Miyazaki [10] and Naito and Nakashizu [11]. Their results indicated that the presence of moderate concentrations of Ni on wafer surfaces before high temperature processing had a greater impact in *p*-type silicon than *n*-type silicon. In both cases their measurements were restricted to one resistivity and a single, undefined, injection-level. In this work we have studied the impact of Ni surface contamination on wafers of different resistivities for both *n*- and *p*-type, and also across a broad range of injection-levels. We have also calculated the surface recombination velocities, a more appropriate metric for the impact of surface precipitates on recombination, from the measured lifetime data. Together, this information provides a more complete characterization of the electronic impact of low to moderate Ni surface contamination.

✉ Fax: +61 2 6125 0506, E-mail: Daniel.Macdonald@anu.edu.au

2 Experimental details

The wafers subjected to Ni contamination were 8 inch Czochralski wafers of ⟨110⟩ orientation and 750 micron thickness, and were prepared by Komatsu. Three resistivities were chosen for both boron-doped *p*-type and phosphorus-doped *n*-type samples, as listed in Table 1. For each of these, four levels of Ni contamination were prepared by dipping into dilute Ni solutions. The resulting Ni concentrations on the wafer surfaces were measured by Total Reflection X-ray Fluorescence (TXRF) and are reported in Table 1. The samples were then annealed at 900 °C for 45 minutes, followed by a slow cooling to 700 °C at a rate of 3 °C/min, at which point they were unloaded and allowed to cool in air. During the anneal at 900 °C the samples were oxidized, resulting in an oxide thickness of 18 nm, which serves as a passivating film to allow sensitive measurement of the carrier lifetime. Control samples of each resistivity were co-processed. These allow the quality of the surface passivation, as well as the impact of any unwanted contamination from the furnace, to be monitored.

Carrier lifetime measurements were performed using the quasi-steady-state photoconductance technique (QSSPC) [12], which allows the effective carrier lifetime to be measured as a function of excess carrier density Δn. In this way the injection-dependence of the carrier lifetime can be examined, which often reveals information about the underlying recombination properties. It also means that different samples can be compared at the same injection level $\eta = \Delta n / N_{\mathrm{dop}}$ where N_{dop} is the dopant concentration. A photographic flash producing white light was used in most cases. For some sam-

Ingot	Resistivity (Ω cm)	dopant density $N_{A/D}$ (cm^{-3})	Ni surf. conc. #1 (cm^{-2})	Ni surf. conc. #2 (cm^{-2})	Ni surf. conc. #3 (cm^{-2})	Ni surf. conc. #4 (cm^{-2})
P1	11	1.2×10^{15}	7.0×10^{10}	3.7×10^{11}	3.3×10^{12}	1.7×10^{13}
P2	14	9.7×10^{14}	7.3×10^{10}	4.2×10^{11}	3.3×10^{12}	1.7×10^{13}
P3	45	3×10^{14}	8.2×10^{10}	3.9×10^{11}	3.3×10^{12}	1.7×10^{13}
N1	2.5	1.9×10^{15}	7.6×10^{10}	3.4×10^{11}	2.9×10^{12}	1.7×10^{13}
N2	11	4.1×10^{14}	8.4×10^{10}	3.4×10^{11}	2.9×10^{12}	1.7×10^{13}
N3	45	1×10^{14}	7.8×10^{10}	3.5×10^{11}	2.9×10^{12}	1.7×10^{13}

TABLE 1 Resistivity, dopant concentration and Ni surface concentration for the samples in this study

ples, we also measured the carrier lifetime using infrared light by placing a silicon wafer of thickness equal to the samples as a filter in front of the flash. This results in a much more uniform generation rate throughout the sample volume, and in comparison with white light measurements, can allow the relative impact of the bulk and the surfaces on the effective lifetime to be partially de-convoluted.

The uncertainty in the absolute values of the measured lifetimes, deriving in turn from uncertainty in the calibration of the inductively-coupled coil, the reference cell, and wafer parameters, are estimated to be between 10%–20%. We will assume 15% as a reasonable figure.

In order to investigate the impact of surface precipitation of the Ni on the measured lifetimes, certain samples were etched in a 1 : 10 HF/HNO_3 solution to a depth of 8 microns per side, and re-passivated with Plasma-Enhanced Chemical-Vapor Deposited (PECVD) SiN films [13].

3 Chemical states of nickel in silicon

Nickel can occur in several forms in crystalline silicon. It may be present in point-like form, occupying either interstitial or substitutional sites in the silicon lattice. It may also occur as precipitates of various chemical make-up. If precipitated heterogeneously, it is likely to form nickel silicide [2]. On the other hand, if precipitated at extrinsic defects such as internal oxygen complexes or oxidized surfaces, it can potentially form silicates as well as silicides.

Ni has a relatively high solid solubility limit in silicon: at 700 and 900 °C, the temperatures of relevance for this work, it is 2.4×10^{15} and 7.4×10^{16} cm^{-3} respectively [14]. In principle, these values can contain contributions from both interstitial and substitutional Ni. However, it has been established that the solubility limit of substitutional Ni is orders of magnitude less than interstitial Ni across the temperature ranges studied here [14, 15]. Note that the maximum surface concentration in Table 1 (1.7×10^{13} cm^{-2}) equates to a volume concentration of around 2×10^{14} cm^{-3} for a thickness of 750 microns. In combination with the very high diffusivity [2] of interstitial Ni (corresponding to a diffusion length of 2.3 mm for 45 minutes at 900 °C) it is therefore clear that the vast majority of the Ni is in interstitial form, and uniformly distributed throughout the wafer thickness, during the annealing used in this study.

Unlike some other metals such as Fe and Cu, Istratov [14] has shown recently that the solubility of Ni is independent of the doping level in both *p*- and *n*-type silicon, courtesy of interstitial nickel's very close proximity to the valence band edge, resulting in a neutral charge state. Consequently, the different types and doping levels in the samples studied here should not affect our assumption that the Ni is almost entirely interstitial during annealing.

However, it is well established that unless extremely rapid quenching is used, virtually all of the interstitial Ni precipitates at the wafer surfaces during cooling [1, 2, 16]. This occurs because of the extremely high diffusivity of interstitial Ni, even at relatively low temperatures where the solubility is greatly reduced, and the fact that nickel silicide forms with almost no strain. Since the samples in this study were cooled relatively slowly in air (as is generally the case during device processing), it is reasonable to expect almost complete precipitation of interstitial Ni at the surfaces. The only Ni likely to remain within the wafer bulk would be substitutional Ni, as it is too immobile to reach the surfaces, but of course due to its very low solubility it must occur at much lower concentrations than the initial interstitial Ni levels.

Both the surface precipitates and the substitutional Ni can in principle contribute to carrier recombination. Among other things, the results of this work shed light on the relative impact of these two forms of Ni, if present, after a more or less standard post-anneal cooling regime.

4 Results and discussion

Figure 1 shows a set of effective carrier lifetime measurements τ_{eff} for the 11 Ω cm *p*-type (P1) samples, including the control and four different pre-anneal surface concentrations of Ni. The white-light data show that the lifetime clearly decreases with increasing Ni concentration. However, the two most lightly Ni contaminated samples are not greatly different to the control sample, especially at higher injection

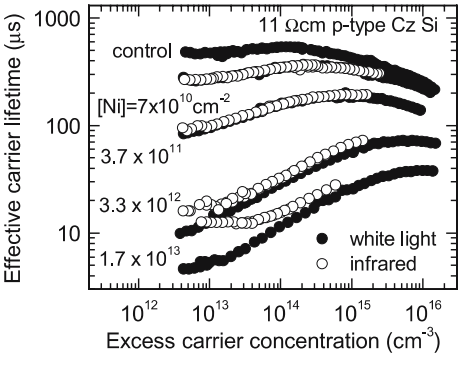

FIGURE 1 Effective carrier lifetime measurements as a function of excess carrier density for the 11 Ω cm *p*-type Cz samples with various Ni surface concentrations prior to annealing. White light and infrared measurements are shown

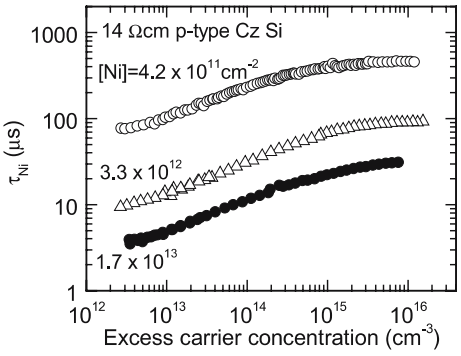

FIGURE 2 The lifetimes due to Ni only, τ_{Ni}, after subtraction of the control data at each excess carrier density, for three of the 14 Ω cm p-type samples, as a function of excess carrier density

levels. To enable us to examine the impact of the Ni alone, without other recombination channels such as oxide interface recombination and Auger recombination (which also occur in the control), we perform a subtraction procedure at each excess carrier density. Assuming that the recombination rates due to the presence of the Ni and these other 'intrinsic' processes are additive, we can determine the lifetime due to the presence of Ni τ_{Ni} as:

$$\frac{1}{\tau_{Ni}} = \frac{1}{\tau_{eff}} - \frac{1}{\tau_{control}} . \quad (1)$$

This procedure requires interpolation of the measured lifetimes between neighboring carrier densities, but due to the high density of data on the carrier density axis this introduces negligible error.

Figure 2 shows the result of this subtraction procedure for the three most heavily contaminated 14 Ω cm p-type samples (P2). The most lightly contaminated sample is not shown due to the large uncertainties generated by subtracting similar values. The results show that the shape of the lifetime curves, which should not depend on the Ni concentration (assuming the chemical state of the Ni is similar in all samples), is now very similar in each case.

4.1 *Location of the Ni-related defects*

At this point it is interesting to consider whether the measured lifetimes are dominated by Ni precipitates at the surfaces, or possibly by substitutional Ni frozen into the wafer bulk. The first evidence to suggest that the surface precipitates dominate comes from a comparison of white light and infrared measurements.

Figure 1 shows the effective lifetimes for the four Ni-contaminated P1 samples measured under both white (causing generation near the surface) and infrared light (causing generation throughout the wafer). Note that the white and infrared data are in close agreement for the two most lightly Ni-doped samples. In these cases, the measured effective lifetimes correspond to carrier diffusion lengths comparable to or greater than the wafer thickness. Therefore the position at which the photo-generation occurs is largely irrelevant, since the carriers can diffuse throughout the entire sample thickness, resulting in a steady-state carrier distribution that is independent of the illuminating wavelength.

In contrast, the more heavily contaminated samples reveal a higher lifetime for infrared light than for white light where the lifetimes are lowest. This can only be explained by a greater recombination rate at the surfaces than in the wafer bulk. Here the surfaces effectively act as a 'sink' for diffusing carriers, meaning that those generated further from the surfaces will persist for longer than those generated near the surface. In the extreme case of an infinite recombination velocity at the surfaces and an infinite bulk lifetime, the measured lifetime would be 16 μs under infrared illumination for a 750 μm thick wafer [17]. This is similar to the lowest infrared values in Fig. 1, suggesting that the actual bulk lifetime may still be quite long in these samples. Hence it seems that the measured lifetimes are indeed dominated by surface precipitates rather than substitutional Ni within the wafer bulk. Similar differences between white light and infrared measurements were observed for the n-type samples.

These conclusions are corroborated by further lifetime measurements after etching approximately 8 microns per side from the samples, then re-measuring the lifetimes after surface passivation with PECVD SiN films. The results are shown in Fig. 3, in the form of carrier lifetimes extracted at an injection level of $\eta = 0.01$. For each type and resistivity, both the controls and the samples with the second heaviest Ni dose are shown, firstly with the existing oxide, and also after etching and SiN passivation. In every case, the control and Ni-contaminated lifetimes are similar after etching, and much higher than prior to etching. This indicates that the majority of the recombination centers have been removed in the surface etching process. Polignano et al. [18] came to the same conclusion after similar etch-back lifetime measurements on Ni-implanted p-type material annealed at 800 °C.

The PECVD SiN method of surface passivation was chosen because it is performed at a relatively low temperature (400 °C), as opposed to thermal oxidation. This should minimize any further changes in the Ni distributions. Nevertheless, it remains a possibility that further precipitation occurred during this deposition, or indeed hydrogenation from the SiN layer may passivate some Ni-related recombination centers. However, in conjunction with the infrared versus white light measurements presented above, the weight of evidence strongly suggests that Ni precipitates at the surface dominate the measured lifetimes, and if any substitutional Ni

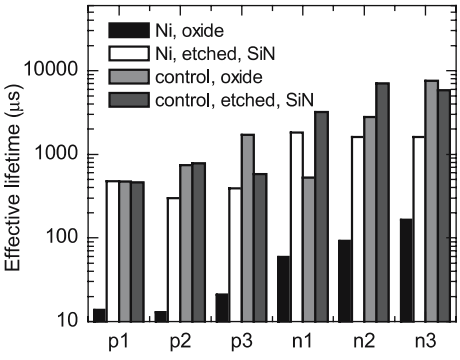

FIGURE 3 Effective lifetimes at an injection level of $\eta = 0.01$ for the second most heavily Ni-contaminated samples of each resistivity, and the controls, before and after etching 8 μm per side. After etching, the surfaces were passivated with PECVD SiN films

exists in the wafer bulk, its impact on the carrier lifetime is minimal. Finally, A. Istratov independently performed Deep-Level Transient Spectroscopy (DLTS) measurements on some identical samples after a shallow surface etch to allow Schottky diode preparation. These revealed little electrical activity attributable to the presence of Ni. This also suggests that most Ni-related recombination centers reside very near the surfaces.

4.2 *Comparison of n- and p-type silicon*

Figures 4 and 5 show the injection dependence of τ_{Ni} for the p-type and n-type samples respectively. The results shown are for the second heaviest Ni surface contamination of around 3×10^{13} cm^{-2}, and after subtraction of the control data. In the p-type samples, the lifetime increases by approximately one order of magnitude from low to high-injection. However, in the n-type samples, the change in lifetime is much less dramatic, and in fact changes from an increasing to decreasing lifetime as the dopant density decreases. Note that in all cases the lifetimes converge to a common value under high injection conditions, as the dopant type or concentration is then immaterial.

Such changes in injection dependence can sometimes be exploited to extract information about capture cross sections of defects [19]. However, from DLTS studies, Ni precipitates are known to produce an extended defect band in the energy gap of silicon [6, 8, 9], although the position of this band is apparently still uncertain [1]. Due to this band-like nature, the standard Shockley–Read–Hall statistics for modeling lifetimes as a function of injection dependence are not applicable, since the cross sections associated with the shallower parts of the band will probably be quite different to the deeper parts. Consequently it was found to be impossible to model the measured curves with a single set of consistent recombination parameters (capture cross sections and energy level). In fact, the injection dependence of the high-resistivity n-type samples reflects the presence of shallower levels, while the behaviour of the p-type samples is more characteristic of the deeper parts of the band. These deeper levels apparently have a larger 'effective' capture cross section for electrons than holes, and dominate the p-type samples, leaving the shallow levels to determine the injection dependence of the n-type samples.

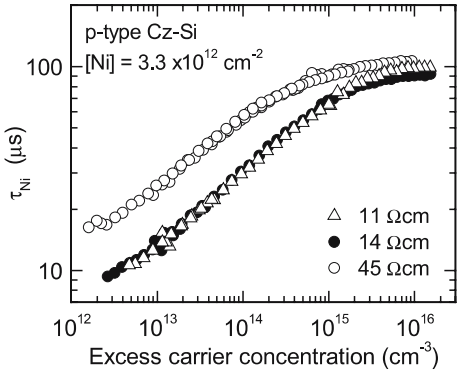

FIGURE 4 The lifetimes due to Ni only, τ_{Ni}, for the three p-type resistivities with the second heaviest Ni contamination, as a function of the excess carrier density

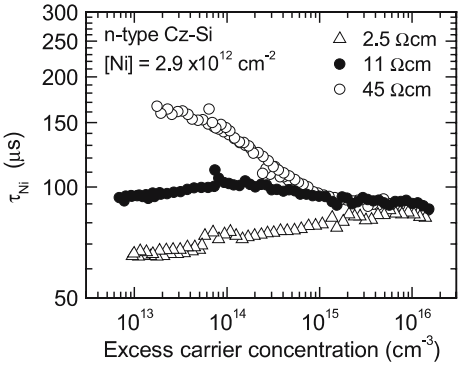

FIGURE 5 The lifetimes due to Ni only, τ_{Ni}, for the three n-type resistivities with the second heaviest Ni contamination, as a function of the excess carrier density

Despite this inability to determine recombination parameters, the results in Figs. 4 and 5 are still interesting from a device perspective, particularly for devices sensitive to recombination such as solar cells. They confirm that n-type silicon is less affected by the presence of Ni precipitates than p-type silicon. A similar preference for n-type silicon has been established for common point-like metal impurities such as Fe, Ti, V, Mo [20]. These metals have larger capture cross sections for electrons than holes, courtesy of their charge state. The reduced impact of Ni precipitates in n-type silicon, in combination with its immunity to other metals, makes this material more attractive for applications such as photovoltaics, in which cheaper, more contaminated source material is a key aspect of cost reduction.

The change in injection-dependence for the n-type samples of Fig. 5 also suggests itself as a possible signature of Ni precipitates. The more heavily and lightly doped samples display opposite injection dependence, while the 11 Ω cm sample has an almost flat injection-dependence. Importantly, the shapes of these curves do not depend on the concentration of Ni precipitates, and would be exhibited by any samples of similar resistivity that were dominated by the presence of Ni precipitates.

Next, in order to more directly compare the impact of the Ni precipitates on wafers of different doping, we have extracted the Ni-related lifetimes at a fixed low-injection level of $\eta = 0.01$. The results for the p- and n-type wafers are shown in Figs. 6 and 7, respectively.

Also shown are the results of Miyazaki [10] (8–12 Ω cm p- and n-type material, spin-coated Ni, annealed at 1000 °C), Naito and Nakashizu [11] (10 Ω cm p- and n-type material, spin-coated Ni, annealed at 1000 °C), and of Polignano et al. [18] (2–20 Ω cm p-type material only, implanted Ni, annealed at 800 °C). In Figs. 6 and 7, we have converted their effective lifetime measurements into the equivalent of our τ_{Ni} by using their control data and (1) (for Miyazaki's data the lowest Ni dose was used in place of a control). We have not attempted to estimate their uncertainties, although for the lower doses, at least, they are likely to be quite large. The injection level used for lifetime measurement was not reported in any of these cases.

The n-type data presented here agree very well with those of Naito and Nakashizu, and also quite well with those of

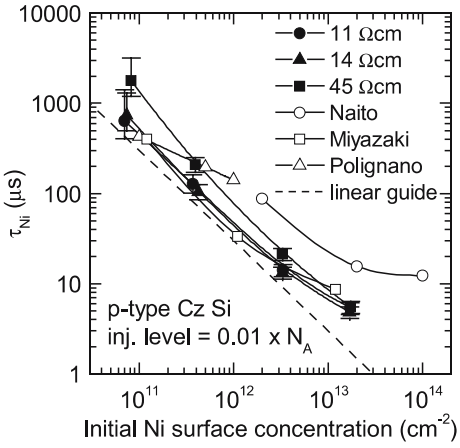

FIGURE 6 τ_{Ni} as a function of the initial Ni surface concentration for the p-type samples at a fixed low injection level of $\eta = 0.01$. Data from Naito and Nakashizu, Miyazaki, and Polignano et al. is shown for comparison. The *dashed line* represents an inverse linear dependence

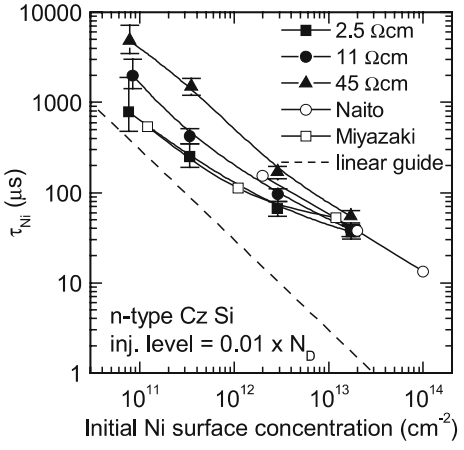

FIGURE 7 τ_{Ni} as a function of the initial Ni surface concentration for the n-type samples at a fixed low injection level of $\eta = 0.01$. Data from Naito and Nakashizu, and Miyazaki is shown for comparison. The *dashed line* represents an inverse linear dependence

Miyazaki. In this case, the specific injection-level used is not so critical, since the injection-dependence of the lifetime is not very pronounced in n-type silicon, as shown in Fig. 5. However, while the p-type data measured here agrees extremely well with Miyazaki's, it is significantly lower than that of Naito and Nakashizu. In addition, our data exhibit a more linear dependence on the Ni dose than the data of Polignano et al. These differences may be due to the injection level used, which is much more important in the p-type samples. In fact, our data extracted at a higher injection level of $\eta = 0.5$ agree very well with those Naito and Nakashizu for both n- and p-type, suggesting their experimental conditions were nearer this value. It may be that different injection levels used by Polignano et al. from sample to sample caused the apparently gentler dependence on the Ni dose. Here we have chosen to represent our data at a fixed lower injection level of $\eta = 0.01$ to more clearly illustrate the differences between n- and p-type silicon. The good agreement with Miyazaki's data implies that a similar injection level was used in that study.

It is notable that in the p-type samples, the decrease in lifetime with increasing Ni concentration is clearly linear for lower Ni levels. At higher Ni levels, τ_{Ni} begins to saturate, in agreement with the data of both Miyazaki and Naito and Nakashizu. Such behavior can result from either a change in the precipitation dynamics, or may in fact be caused by a transport-limited measurement artifact.

Regarding the precipitation dynamics, a linear decrease in the lifetime with dose implies that the number of precipitates per unit volume also increases linearly, while their size does not change significantly with dose. On the other hand, a strongly sub-linear response to the dose suggests that the density of precipitates has begun to saturate, and extra Ni tends to increase their size, rather than form new precipitates. However, such speculation would need to be confirmed by direct observation of the precipitate size and distribution.

However, before reaching this conclusion, it must be acknowledged that saturation of the effective lifetime with Ni dose may reflect the transport-limited nature of lifetime measurements in thick wafers with high surface recombination rates. Even with the most severe surface recombination, several microseconds can still be measured due to the time required for carriers to reach the surfaces, and this lifetime increases with the sample thickness. This is discussed further in the following section, in which the surface recombination velocities are calculated from the measured effective lifetimes.

In the n-type samples of Fig. 7, a primary observation is that the magnitudes of the lifetimes are considerably higher than in the p-type samples, in agreement with the findings of Miyazaki, and also those of Naito and Nakashizu (although theirs were less pronounced due to the higher injection level apparently used). Secondly, there is a considerable difference in the lifetimes of the various n-type resistivities. This is a direct consequence of the changing injection dependence of Ni precipitates in n-type silicon as the resistivity moves above or below approximately 10 Ω cm. Finally, the data suggest that the dose-dependence is somewhat sub-linear for the more heavily doped n-type samples, while being approximately linear for the 45 Ω cm material. This could indicate an earlier shift to increasing precipitate size, rather than increasing density, in these samples. Such an effect could be related to the higher Fermi-level in the more heavily doped n-type wafers compared to the other samples, resulting in a greater amount of negative charge on the precipitates, in turn possibly affecting their propensity to bind excess Ni.

Figure 8 shows the results for all samples in high-injection conditions, $\eta = 10$. In this case, all samples give similar results, as expected since the doping type and level is then of little consequence. The approximately linear dependence of τ_{Ni} on dose for lower Ni concentrations, and the saturation at higher Ni levels, is again reflected in this data.

Finally, it is interesting to compare the relative impact of Ni contamination to other common metal impurities. As an example, a surface concentration of 10^{11} cm^{-2} of Fe diffused uniformly throughout a 750 μm thick wafer would result in a minority carrier lifetime of just 10 μs at an injection level of $\eta = 0.01$ in 10 Ω cm p-type silicon, if present as interstitial Fe [21]. The equivalent value for Ni precipitates from Fig. 6 is around 700 μs. This is consistent with the findings of Hopkins and Rohatgi [22], who found that a p-type Cz solar cell process could tolerate between one and two orders of

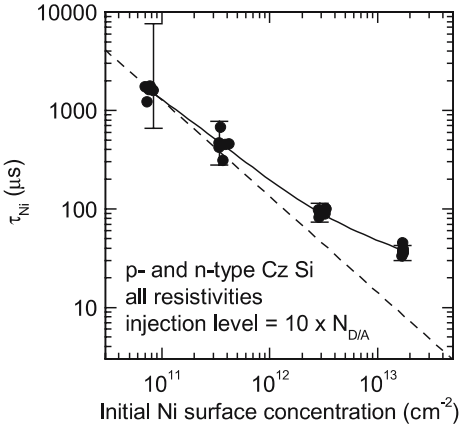

FIGURE 8 τ_{Ni} as a function of the initial Ni surface concentration for all n- and p-type samples at a fixed high injection level of $\eta = 10$. The *dashed line* represents an inverse linear dependence

magnitude more Ni than Fe, although their impurities were grown into the crystal, rather than occurring as surface contaminants. The recombination activity of a given amount of surface Ni contamination is also relatively low in comparison to other metals such Cr, Ti, Mo and V [20], which, like Fe, also tend to remain in interstitial form after standard cooling conditions, rather than segregating to the surface and precipitating as Ni does.

4.3 *Surface recombination velocities*

As Polignano et al. have pointed out [18], when discussing the impact of surface precipitates on carrier recombination, it is, strictly speaking, more correct to characterize the results in terms of surface recombination velocities than effective lifetimes. Such an approach has the advantage of allowing the transport-related artifact that can cause the effective lifetime to saturate with dose, and discussed above, to be effectively removed.

To this end, we have calculated the surface recombination velocities S (cm/s) from the effective lifetime measurements under the so-called steady-state approximation [23]. This approach yields accurate results over the range of parameters used here, even for cases with high surface recombination velocities and low effective lifetimes when carrier transport can restrict the surface recombination rate, as shown by Brody et al. [23]. For these calculations we used data measured with infrared illumination and assumed uniform generation profiles. For the cases where the surface recombination velocity was sufficiently low to be unaffected by transport constraints (< 100 cm/s for the p-type samples and < 30 cm/s for the n-type samples), the calculations agreed very well with values determined via the simplified expression $1/\tau_{\text{eff}} = 1/\tau_{\text{b}} + 2S/W$, where τ_{b} is the bulk lifetime and W the wafer thickness. The bulk lifetime was taken as the effective lifetimes measured after etching the near-surface region and re-passivating with SiN films, and extracted at the required injection-level. These were among the highest lifetimes measured for each resistivity throughout this study, but nevertheless only give a lower bound on the true bulk lifetime. As such, the surface recombination velocities calculated are in fact upper bounds.

Figures 9 and 10 show the results for the p-type and n-type samples respectively, at an injection level of $\eta = 0.01$. In the p-type case, the uncertainties are large for the higher surface recombination velocities, but nevertheless the S values follow an approximately linear trend with Ni dose. For doses above 10^{13} cm^{-2}, the surface recombination velocity becomes effectively infinite in the p-type samples.

The S values are significantly lower in the n-type samples, as implied by the lifetime measurements, and there is again a clear distinction between the different resistivities. The linear trend of the highest resistivity sample is clear, but once again the more heavily doped n-type samples have a slightly sub-linear response.

Note that the linear trends in the p-type case and the lightly-doped n-type case hold even for the higher Ni doses, unlike the effective lifetime data of Figs. 6 and 7. This is consistent with the Ni precipitates increasing primarily in number, but not in size, over the whole Ni range studied. This highlights the importance of characterizing the recombination activity of surface precipitates as recombination velocities, rather than lifetimes, especially for heavily-contaminated and relatively thick samples in which transport limitations can make effective lifetime measurements artificially high.

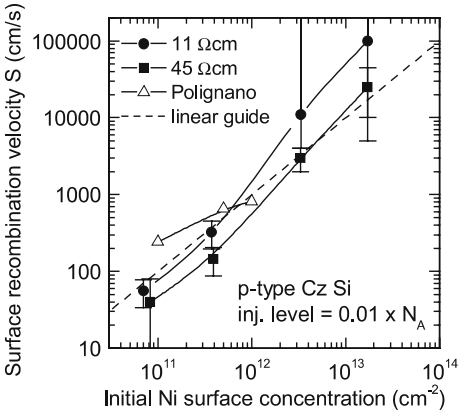

FIGURE 9 Surface recombination velocity S as a function of the initial Ni surface concentration for the p-type samples at a fixed low injection level of $\eta = 0.01$. Data from Polignano et al. is shown for comparison. The *dashed line* represents a linear dependence

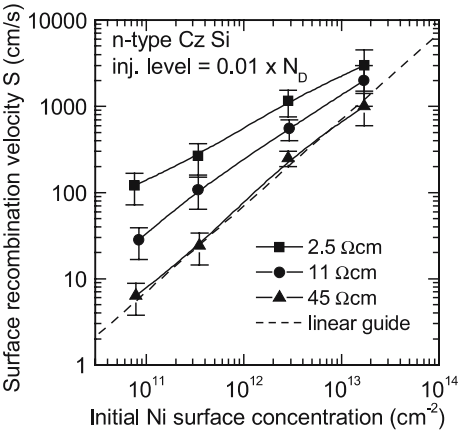

FIGURE 10 Surface recombination velocity S as a function of the initial Ni surface concentration for the n-type samples at a fixed low injection level of $\eta = 0.01$. The *dashed line* represents a linear dependence

Finally, the samples used in this study were of ⟨110⟩ orientation. Although Ni is expected to precipitate at the surfaces for any orientation [2], its impact on the surface recombination velocity may be different for other orientations. For example, uncontaminated ⟨100⟩ oriented samples generally yield lower surface recombination velocities due to a lower areal density of unsatisfied bonds. In this case, the degradation in surface recombination velocity due to Ni precipitates may be greater than for ⟨110⟩ wafers.

5 Conclusions

Carrier lifetime studies have shown that the dominant Ni-related recombination centers after high temperature processing followed by air-cooling are Ni precipitates at the wafer surfaces. These are formed by the rapid diffusion of interstitial Ni to the surfaces during cooling. The results confirm that surface Ni precipitates have a greater impact on carrier lifetimes in p-type silicon than n-type under low- and moderate-injection conditions. These observations may be of significance for devices sensitive to recombination such as solar cells, although, per atom, the effect of Ni contamination is significantly less than other interstitial metals such as Fe. The presence of the precipitates may also be relevant for surface field-effect devices such as MOSFETs.

The reduced lifetimes caused by the Ni precipitates were found to depend more strongly on the wafer doping level for n-type Si than p-type, despite their lesser impact in this material. In fact, the observed change in the shape of the injection-level dependence of the effective lifetimes in n-type samples of resistivity around 10 Ω cm may be a useful characteristic signature of Ni precipitates. Finally, calculations of the surface recombination velocity suggest that the recombination activity of the Ni precipitates at oxidized surfaces increases approximately linearly with the Ni dose. This linear response contrasts with the effective lifetime measurements, which are affected by transport-limited artifacts at higher Ni doses. The exception to this observation was the more heavily-doped n-type samples, which show a sub-linear behavior, which may reflect altered precipitation dynamics related to the position of the Fermi level.

ACKNOWLEDGEMENTS The Ni contaminated samples were prepared by A. Andrukhiv and K. Nagai of Komatsu, and A.A. Istratov of the University of California, Berkeley, who very kindly made them available to the author, and who contributed many helpful suggestions. The author is grateful to C. Jagadish and H. Tan of Electronic Materials Engineering, ANU, for access to the PECVD reactor, and to A. Cuevas for insightful suggestions. This work has been supported by the Australian Research Council.

REFERENCES

1 A.A. Istratov, E.R. Weber: Appl. Phys. A **66**, 123 (1998)
2 K. Graff: *Metal Impurities in Silicon-Device Fabrication, Springer Series in Material Science* (Springer-Verlag, Berlin, 2000)
3 S.A. McHugo, A.C. Thompson, A. Mohammed, G. Lamble, I. Perichaud, S. Martinuzzi, M. Werner, M. Rinio, W. Koch, H.U. Hoefs, C. Haessler: J. Appl. Phys. **89**, 4282 (2001)
4 O.F. Vyvenko, T. Buonassisi, A.A. Istratov, H. Hieslmair, A.C. Thompson, R. Schindler, E.R. Weber: J. Appl. Phys. **91**, 3614 (2002)
5 A.A. Istratov, T. Buonassisi, R.J. McDonald, A.R. Smith, R. Schindler, J.A. Rand, J.P. Kalejs, E.R. Weber: J. Appl. Phys. **94**, 6552 (2003)
6 W. Schröter, J. Kronewitz, U. Gnauert, F. Riedel, M. Siebt: Phys. Rev. B **52**, 13 726 (1995)
7 F. Riedel, J. Kronewitz, U. Gnauert, M. Siebt, W. Schröter: Solid State Phenomena **47–48**, 359 (1996)
8 H. Hedemann, W. Schröter: Solid State Phenomena **57–58**, 293 (1997)
9 O.F. Vyvenko: Solid State Phenomena **63–64**, 301 (1998)
10 M. Miyazaki: In: *Recombination Lifetime Measurements in Silicon, ASTM STP 1340*, ed. by D.C. Gupta, F.R. Bacher, W.M. Hughes (American Society for Testing and Materials, West Conshohocken, 1998), p. 294
11 S. Naito, T. Nakashizu: In: *Materials Research Society Symposium Proceedings, Defect Engineering in Semiconductor Growth, Processing and Device Technology,* (Materials Research Society, 1992), p. 641
12 R.A. Sinton, A. Cuevas: Appl. Phys. Lett. **69**, 2510 (1996)
13 M.J. Kerr, A. Cuevas: Semicond. Sci. Technol. **17**, 166 (2002)
14 A.A. Istratov, P. Zhang, R.J. McDonald, A.R. Smith, M. Seacrist, J. Moreland, J. Shen, R. Wahlich, E.R. Weber: J. Appl. Phys. **97**, 023 505 (2005)
15 H. Lemke: Phys. Status Solidi A **99**, 205 (1987)
16 E.R. Weber: Appl. Phys. A **30**, 1 (1983)
17 A. Cuevas, R.A. Sinton: Progress in Photovoltaics **5**, 79 (1997)
18 M.L. Polignano, F. Cazzaniga, A. Sabbadini, G. Queirolo, A. Cacciato, A.D. Bartolo: Mater. Sci. Eng. **B42**, 157 (1996)
19 S. Rein, T. Rehrl, W. Warta, S.W. Glunz: J. Appl. Phys. **91**, 2059 (2002)
20 D. Macdonald, L.J. Geerligs: Appl. Phys. Lett. **85**, 4061 (2004)
21 D. Macdonald, A. Cuevas, J. Wong-Leung: J. Appl. Phys. **89**, 7932 (2001)
22 R.H. Hopkins, A. Rohatgi: J. Cryst. Growth **75**, 67 (1986)
23 J. Brody, A. Rohatgi, A. Ristow: Solar Energy Mater. Solar Cells **77**, 293 (2003)